The Astrophysical Journal, 944:153 (5pp), 2023 February 20 https://doi.org/10.3847/1538-4357/acb3c3

The Impact of Spin-kick Alignment on the Inferred Velocity Distribution of Isolated Pulsars

Ilya Mandel[1,2] and Andrei P. Igoshev[3]
[1] School of Physics and Astronomy, Monash University, Clayton, Victoria 3800, Australia; ilya.mandel@monash.edu
[2] The ARC Center of Excellence for Gravitational Wave Discovery—OzGrav, Australia
[3] Department of Applied Mathematics, University of Leeds, LS2 9JT Leeds, UK
Received 2022 October 21; revised 2023 January 8; accepted 2023 January 13; published 2023 February 21

Abstract

The speeds of young isolated pulsars are generally inferred from their observed 2D velocities on the plane of the sky under the assumption that the unobserved radial velocity is not special, i.e., that the measured 2D velocity is an isotropic projection of the full 3D velocity. However, if pulsar spins are preferentially aligned with kicks, then the observer's viewing angle relative to the pulsar velocity vector is in fact special because the direction of the spin impacts the detectability of the pulsar. This means that the measured 2D velocity of observable pulsars is not an isotropic projection, which affects inference on 3D velocities. We estimate this effect and conclude that it could lead to a $\sim$15% systematic overestimate of neutron-star natal kicks if young pulsars have high obliquity angles and narrow beams, but the exact correction factor depends on the distribution of beam-spin and spin-kick misalignment angles and beam widths.

Unified Astronomy Thesaurus concepts: Neutron stars (1108); Pulsars (1306); Radio pulsars (1353)

1. Introduction

The natal kick velocities of neutron stars play a key role in a number of physical processes, from their retention in globular clusters to the evolution of binaries, ranging from neutron-star X-ray binaries to gravitational-wave sources (e.g., Sigurdsson 2003; Bray & Eldridge 2016; Igoshev et al. 2021; Mandel et al. 2021). Over the last twenty years, a number of studies inferred the pulsar velocity distribution from the increasingly large and accurately measured sample of observed single pulsar velocities (e.g., Arzoumanian et al. 2002; Hobbs et al. 2005; Faucher-Giguère & Kaspi 2006; Verbunt et al. 2017; Igoshev 2020).

Generally only the radio pulsar location and the 2D velocity projected onto the plane of the sky can be measured. Therefore, most of these studies had to assume that the measured 2D velocities are isotropic projections of the true 3D velocity. Verbunt et al. (2017) and Igoshev (2020) explored semi-isotropic velocity distributions as well: they assumed that the total 3D velocity points away from the Galactic plane for young radio pulsars. (Because the dynamical timescale in the Galactic potential is $\sim$100 Myr at our distance of 8 kpc from the Galactic center, acceleration can be neglected for young pulsars with ages $\lesssim$10 Myr; we therefore also focus on young pulsars in this work.) Radio pulsar progenitors are massive stars born in the thin Galactic disk. Pulsars are ejected from the disk by natal kicks. A young pulsar with a significant height above the thin disk is likely moving in the same direction, i.e., away from the Galactic plane.

Here, we consider a previously unappreciated selection effect (see, e.g., Lorimer et al. 1997 for a detailed discussion of other relevant selection effects in inferring pulsar velocities). There is a growing body of observational evidence that spins and velocities of pulsars are preferentially aligned (Johnston et al. 2005; Wang et al. 2006; Postnov & Kuranov 2008; Noutsos et al. 2013; Yao et al. 2021). Meanwhile, Janka et al. (2022) proposed that supernova fallback would naturally explain the alignment of the spin axis with the kick direction though the neutrino-induced kick models of Coleman & Burrows (2022) show a weaker antialignment. If pulsar spins are indeed aligned with their kicks, then the detectability of the pulsar, which depends on the location of the observer relative to the spin axis, implies that the radial component of the velocity distribution of *detectable* pulsars follows a different distribution than the components perpendicular to the line of sight.[4]

Here, we evaluate the implications of the anisotropy in the velocities of detectable pulsars on the inference of true pulsar speeds from their observed 2D velocities. Below, we employ toy models to demonstrate the impact of this anisotropy and estimate its potential effect. We do not reanalyze the pulsar sample, which would require a choice of the shape of the kick velocity distribution (see Igoshev 2020; Kapil et al. 2022), a forward model for pulsar evolution in the Galaxy, and careful accounting for observational errors and selection effects (Arzoumanian et al. 2002).

2. Methodology and Motivation

We assume that the pulsar velocity is approximately aligned with the spin vector, with misalignment angle $\gamma \ll 1$ (this does not account for the acceleration of the pulsar in the Galactic potential and is therefore relevant only for young pulsars). We consider a simple bipolar conical beam, with half-opening angle $\beta \leqslant \pi/2$, whose axis is misaligned by an angle $\alpha \leqslant \pi/2$ from the spin axis. We consider an observer viewing the pulsar

[4] Our assumption that the pulsar's velocity closely follows the natal kick is predicated on the fact that the typical kicks are much larger than the peculiar velocity of the progenitor star, including the velocity due to orbital motion if the pulsar is ejected from a wide binary (e.g., Kapil et al. 2022), and that subsequent acceleration in the Galactic potential does not significantly change the velocity for young pulsars.

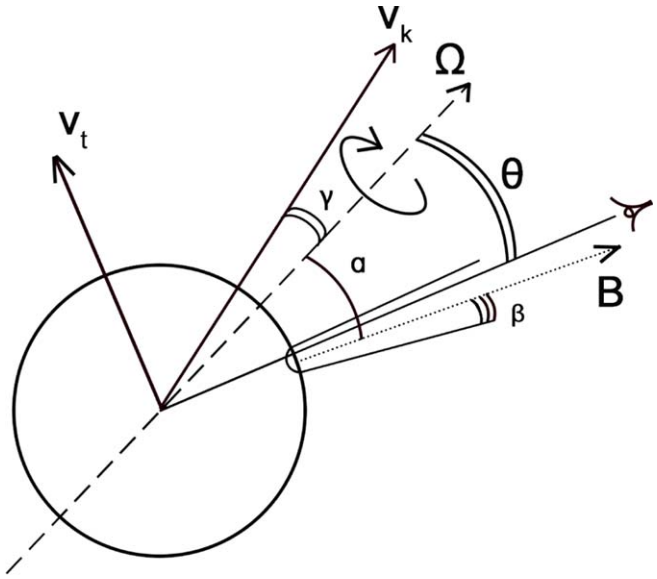

Figure 1. Sketch of the angles in the problem. The pulsar velocity v_k is assumed to be misaligned from the spin axis by a small angle γ; $\alpha \leqslant \pi/2$ is the angle between the beam center and the spin axis; $\theta \leqslant \pi/2$ is the angle between the observer and the spin axis so that v_t is the velocity transverse to the line of sight; β is the half-opening angle of each of the bipolar, conical beams.

from an angle θ off the spin axis (which can also be assumed to be $\leqslant \pi/2$ without loss of generality for a bipolar beam). The setup is illustrated in Figure 1.

In order for a radio source to be discovered and classified as a radio pulsar, it must have detectable *pulsed* emission. We therefore require that the observer must at least sometimes, but not always, be inside the beam. This is satisfied if and only if the following four conditions are met: (i) $\theta < (\alpha + \beta)$; (ii) $\theta < \pi - (\alpha + \beta)$; (iii) $\theta > (\alpha - \beta)$; and (iv) $\theta > (\beta - \alpha)$. (Note that several of these will be met trivially—e.g., if $\alpha > \beta$, condition (iv) is automatically satisfied, while if $\alpha < \beta$, condition (iii) is automatically satisfied.)

We can now ask the question of how the 2D observable pulsar velocity distribution would differ from the isotropically projected 2D velocity distribution for different choices of α and β.

Generally, we expect that if the beams are closely aligned with the spin axis ($\alpha \ll \pi/2$) and are moderately narrow (small β), only observers looking nearly along the spin axis (small θ) will be able to detect the pulsar. Consequently, if the spin is aligned with the velocity, such observers will see a significantly reduced projection of the total speed onto the plane of the sky. The proper motions of detectable pulsars with closely aligned velocities and magnetic dipoles will nearly vanish. The full speeds inferred from the 2D speeds under the assumption of isotropy could then be greatly underestimated.

On the other hand, if moderately narrow beams are significantly misaligned from the spin axis ($\alpha \to \pi/2$), only observers who are also at nearly right angles to the spin axis ($\theta \to \pi/2$) will be able to detect the pulsar. Such observers would see nearly the full velocity vector projected onto the plane of the sky, so their observed 2D velocity distribution will be greater than under the isotropic assumption. The full pulsar speeds inferred from 2D speeds under the assumption of isotropy would be overestimated in this case. The overestimate for $\alpha \to \pi/2$, $\beta \to 0$, and $\gamma \to 0$ has a maximum of $\sqrt{3}/\sqrt{2} \approx 1.22$.

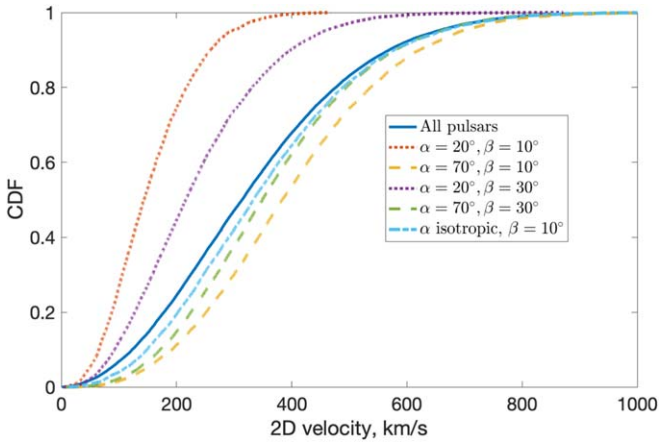

Figure 2. The CDFs of 2D velocity projections of all pulsars sampled from a Maxwellian distribution with $\sigma = 265\ \mathrm{km\ s^{-1}}$ (dark blue) and the subset of detectable pulsars under varying assumptions about the beam misalignment angle α and the beam half-width β, with $\gamma = 0$ (see Section 2).

Moreover, narrower beams (smaller β) will show a stronger selection effect, which should be progressively washed out as the beamwidth increases (larger β).

We illustrate these points in Figure 2. For illustrative purposes only, we sample the 3D speed following a Maxwellian distribution with 1D root mean square velocity dispersion $\sigma = 265\ \mathrm{km\ s^{-1}}$, following Hobbs et al. (2005). We consider pulsar velocities perfectly aligned with the spin axis, $\gamma = 0$. The observer's location is not a priori special, so the angle θ is isotropically distributed: $p(\theta) = \sin\theta$. We consider several different combinations of α and β. We plot the cumulative distribution functions (CDFs) of projected 2D velocities of all pulsars, ignoring selection effects, in solid blue. Other CDF curves show the 2D velocities for pulsars that are considered detectable according to the conditions specified above.

As expected, large misalignment angles $\alpha = 70°$ (green and yellow dashed curves) shift the observed 2D distribution upward, while small misalignment angles $\alpha = 20°$ (red and purple dotted curves) shift it downward. Moreover, in line with expectations, the shifts are greater for narrow beams with $\beta = 10°$ (red, yellow) than wide beams with $\beta = 30°$ (purple, green). In light blue, we show the case of narrow ($\beta = 10°$) beams with isotropically distributed misalignment angles, $p(\alpha) = \sin\alpha$. Because this distribution prefers more misaligned beams, the 2D velocities are shifted higher than under the assumption of no selection effects.

3. Simplified Population Synthesis

In this section, we illustrate the impact of the anisotropy in the velocities of detectable pulsars with respect to the observer's line of sight on natal kick inference. In order to do this, we assume that the true pulsar velocities follow a Maxwellian distribution. This is partially motivated by, e.g., Hobbs et al. (2005), who fit all observed pulsar velocities to a Maxwellian with $\sigma = 265\ \mathrm{km\ s^{-1}}$, and by Igoshev (2020), who found that the high-velocity component of the pulsar distribution can be fit to a Maxwellian with $\sigma = 336\ \mathrm{km\ s^{-1}}$. Conveniently, under the assumption of a Maxwellian distribution with isotropic velocities and the absence of measurement errors, the maximum-likelihood value of σ can be inferred

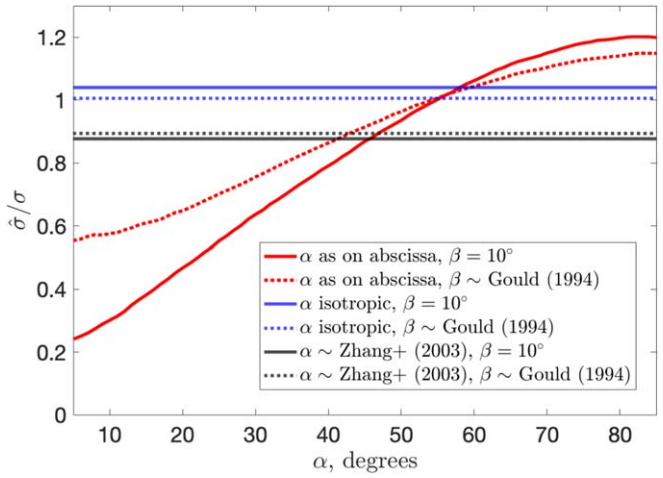

Figure 3. The multiplicative bias of the inferred Maxwellian velocity distribution parameter $\hat{\sigma}$ relative to its true value σ when an isotropic projection of 3D velocity is assumed for inference, without accounting for velocity-direction-correlated selection effects.

directly from the root mean square of the observed 2D velocities as follows.

If measurements are perfect,[5] the likelihood of an individual observation is just the probability distribution from which it is drawn, assumed to be the 2D Maxwellian probability distribution if the pulsar velocities are isotropic:

$$p(v_{2D}|\sigma) = \frac{v_{2D}}{\sigma^2}\exp\left[-\frac{v_{2D}^2}{2\sigma^2}\right]. \quad (1)$$

The likelihood of a set of independent 2D pulsar velocity observations $\{v_{2D}^i\}$ for $i \in [1, N]$ is given by the product of individual likelihoods, so the log-likelihood can be written as a sum:

$$\log \mathcal{L}(\sigma) = \sum_{i=1}^{N} \log p(v_{2D}^i|\sigma). \quad (2)$$

In this simple case, the log-likelihood can be optimized analytically:

$$\frac{\partial \log \mathcal{L}}{\partial \sigma} = -\frac{2N}{\sigma} + \frac{1}{\sigma^3}\sum_{i=1}^{N}(v_{2D}^i)^2 = 0. \quad (3)$$

Hence the maximum likelihood estimate of σ is

$$\hat{\sigma} = \sqrt{\frac{\langle v_{2D}^2\rangle}{2}}, \quad (4)$$

where $\langle v_{2D}^2\rangle$ is the mean value of squared 2D speeds.

In order to evaluate the impact of anisotropy among detectable pulsars, we draw a mock population of pulsars with natal kicks sampled from a Maxwellian distribution with parameter σ, determine if they are detectable as described in the previous section from the perspective of an observer placed at a random isotropically chosen observer angle θ, $p(\theta) = \sin\theta$, compute the transverse velocities $v_{2D} = v\sin\theta$ for the detectable pulsars, and evaluate the systematic bias in the inferred maximum-likelihood parameter $\hat{\sigma}$ under the assumption of isotropy in the pulsar velocity, $\hat{\sigma}/\sigma$.

In Figure 3, we plot the bias $\hat{\sigma}/\sigma$ as a function of the misalignment angle α for $\beta = 10°$ in solid red. As suggested by Figure 2 and the associated discussion, α has a very strong impact on the 2D velocities of detectable pulsars, with larger α leading to larger projected velocities and hence, overestimation of the true velocity dispersion when an isotropic velocity distribution is assumed.

We indeed find that large misalignments between the beam and the spin/kick axis ($\alpha \to \pi/2$) lead to a $\sim$15% systematic overestimate of the underlying kick velocity as parameterized by σ. Conversely, low misalignment angles $\alpha \to 0$ could lead to the underlying natal kick velocity distribution being underestimated by up to a factor of 4, as most detectable pulsars would be viewed nearly on-axis, with transverse velocities strongly suppressed.

Of course, in a realistic pulsar population, α and β are not fixed but follow some distributions, which we assume are independent of each other and of the kick velocity (but see, e.g., Faucher-Giguère & Kaspi 2006 for further discussions). For the beam radius β, we use a relationship between β and the initial pulsar period P_0 fit by Gould (1994; see also Tauris & Manchester 1998):

$$\beta(P_0) = 5°.4\left(\frac{P_0}{1\ \mathrm{sec}}\right)^{-1/2}. \quad (5)$$

We follow Igoshev et al. (2022) in drawing the periods of young pulsars from a log-normal distribution with $\mu_{\log(P/s)} = -1.04$ and $\sigma_{\log P} = 0.53$ for periods in the range $P_0 \in [0.01, 2]$ s. This leads to a mean $\langle\beta\rangle \approx 20°$, larger than the fixed value of 10° assumed previously. Following the analysis in Section 2, we expect larger β to reduce the bias in the inferred velocity, which is exactly what we see in Figure 3, where dotted curves indicate β sampled according to Equation (5).

We also consider two distributions for the obliquity angle α. The systematic bias for a population with an isotropic distribution of α is indicated with a blue horizontal line in Figure 3. As expected from the minimal shift in the 2D velocity CDFs in Figure 2, an isotropic α distribution leads to very small biases of 4% (0.5%) in the recovered σ for $\beta = 10°$ (β from Equation (5)).

The distribution of the obliquity angle α has been estimated for hundreds of radio pulsars (Lyne & Manchester 1988; Rankin 1993a, 1993b). Tauris & Manchester (1998) combined these measurements to argue that the distribution of α is not uniform and peaks at lower values. Zhang et al. (2003) proposed the following probability density function:

$$p(\alpha) = \frac{0.784}{\cosh(3.5[\alpha - 0.43])} + \frac{0.294}{\cosh(4[\alpha - 1.6])}, \quad (6)$$

where $\alpha \in [0, \pi/2]$. This fit does indeed support lower values of α, with a peak around 25°, and we may thus expect that a population that follows this α distribution would lead to an underestimate of the pulsar velocity distribution. Indeed, we find that the velocity distribution is underestimated by 12% (11%) for $\beta = 10°$ (β from Equation (5)) as shown in black in Figure 3.

Y. Yuri Levin (2022, private communication) suggested a possible test of the consistency of this model. Pulsars with

[5] Real pulsar velocity measurements are, of course, not perfect, nor are pulsar velocities drawn from a single Maxwellian distribution (e.g., Igoshev 2020; Kapil et al. 2022), so this calculation is only intended to indicate the likely size of the effect.

lower 2D velocities should be the ones preferentially viewed close to the spin axis in this model. They should then have larger pulse duty cycles. However, we find that our theoretical models predict only moderate anticorrelations between the 2D observed velocities and the pulse duty cycle, estimated as $\sqrt{\beta^2-(\alpha-\theta)^2}\big/(\pi\sin\theta)$. For example, we predict the Pearson correlation coefficient between the pulse duty cycle and 2D speed of detectable pulsars to be -0.3 for the Zhang et al. (2003) α distribution and the β distribution from Equation (5) but nearly zero for $\alpha=75^\circ$ and $\beta=10^\circ$. Moreover, the sampling scatter in this correlation coefficient from a small sample of 80 pulsars—the number for which very long baseline interferometry (VLBI) parallax and proper motions data are available (see Table A1 in Igoshev 2020)—is quite large (e.g., 0.13 in the latter example). The model is thus consistent with the measured correlation coefficient of -0.13 between the pulse duty cycle and the 2D velocities of pulsars with VLBI data. Here, the pulse duty cycle is computed as the ratio between the width at 50% amplitude, obtained from the ATNF pulsar catalog[6] (Manchester et al. 2005), and the pulsar period. While consistent, this test is inconclusive.

4. Implications

We have shown that if young pulsars have natal kicks aligned (or anti-aligned) with their spins, then the distribution of observed 2D velocities of detectable pulsars may be systematically shifted relative to isotropic projections of pulsar 3D speeds onto the plane of the sky (see Figure 2). Consequently, the 3D speed distribution inferred from the observed 2D velocities could be systematically biased (see Figure 3).

The size of the bias strongly depends on the distribution of the pulsar obliquity angle α and pulsar beam size β. A preference for small obliquity angles found by, e.g., Tauris & Manchester (1998), would suggest that pulsar 3D speeds are $\sim$10% larger than inferred in previous studies, based on the Zhang et al. (2003) fit to the α distribution. However, this fit was incorrectly derived by using the Kolmogorov–Smirnov test statistic as a form of likelihood. Of course, this test should only be used to accept or reject a particular hypothesis and cannot be used to compare acceptable hypotheses against each other.

Perhaps a more serious issue is that both α and β appear to evolve as the pulsar ages. For example, Figures 5 and 6 of Tauris & Manchester (1998) show, based on the data of Gould (1994) and Rankin (1993a), that pulsars become more aligned over time, matching theoretical expectations (e.g., Goldreich 1970; Philippov et al. 2014). Conversely, young pulsars should have larger misalignment angles than the overall pulsar population. Studies of pulsar kick angles typically rely on young pulsars (e.g., Igoshev 2020; Willcox et al. 2021; Kapil et al. 2022), which may thus have preferentially larger α, possibly leading to a $\sim$15% overestimate in the inferred kick velocities after accounting for the wider beams of younger pulsars (Gould 1994; Tauris & Manchester 1998). This effect could be reduced if the alignment between pulsar kicks and spins is imperfect ($\gamma>0$).

Velocities are inferred from the analysis of young pulsars because older pulsars exhibit signs of acceleration in the Galactic potential, so their current velocities no longer reflect their natal velocity kicks. This also means that the effect we describe in this paper would disappear for older pulsars as pulsar acceleration would change the velocity orientation relative to the original kick direction while leaving the spin direction intact, destroying the spin-kick alignment. Indeed, Noutsos et al. (2013) noted that the correlation between the orientation of the proper motion and spin axis of a pulsar disappears for objects with kinematic ages above 10 Myr.

Furthermore, these considerations apply only to nonrecycled pulsars. The spin direction of a recycled pulsar is set by the orbital angular momentum of its host binary. While the velocities of such binaries, or pulsars ejected from the binaries, may be correlated to the orbital plane (e.g., some kick directions are more or less likely to disrupt the binary), this is likely a less significant effect.

In summary, if young pulsars have kicks preferentially aligned with their spins, large obliquities, and relatively narrow beams, then their 3D speeds may typically be $\sim$15% lower than the values inferred from observed 2D transverse velocities without considering the effect discussed in this paper. Reduced natal kicks would make it easier to retain the observed pulsar population in globular clusters and preserve a higher fraction of neutron-star binaries, including X-ray binaries and future gravitational-wave sources, from disruption during supernovae.

We thank Yuri Levin and Matthew Bailes for useful discussions. I.M. acknowledges support from the Australian Research Council Centre of Excellence for Gravitational Wave Discovery (OzGrav), through project number CE17010004. I. M. is a recipient of the Australian Research Council Future Fellowship FT190100574. Part of this work was performed at the Aspen Center for Physics, which is supported by National Science Foundation grant PHY-1607611, with I.M.'s participation partially supported by the Simons Foundation. The work of A.P.I. is supported by STFC grant No. ST/S000275/1.

ORCID iDs

Ilya Mandel https://orcid.org/0000-0002-6134-8946
Andrei P. Igoshev https://orcid.org/0000-0003-2145-1022

References

Arzoumanian, Z., Chernoff, D. F., & Cordes, J. M. 2002, ApJ, 568, 289
Bray, J. C., & Eldridge, J. J. 2016, MNRAS, 461, 3747
Coleman, M. S. B., & Burrows, A. 2022, arXiv:2209.02711
Faucher-Giguère, C.-A., & Kaspi, V. M. 2006, ApJ, 643, 332
Goldreich, P. 1970, ApJL, 160, L11
Gould, D. M. 1994, PhD thesis, Univ. of Manchester
Hobbs, G., Lorimer, D. R., Lyne, A. G., & Kramer, M. 2005, MNRAS, 360, 974
Igoshev, A. P. 2020, MNRAS, 494, 3663
Igoshev, A. P., Chruslinska, M., Dorozsmai, A., & Toonen, S. 2021, MNRAS, 508, 3345
Igoshev, A. P., Frantsuzova, A., Gourgouliatos, K. N., et al. 2022, MNRAS, 514, 4606
Janka, H.-T., Wongwathanarat, A., & Kramer, M. 2022, ApJ, 926, 9
Johnston, S., Hobbs, G., Vigeland, S., et al. 2005, MNRAS, 364, 1397
Kapil, V., Mandel, I., Berti, E., & Müller, B. 2022, arXiv:2209.09252
Lorimer, D. R., Bailes, M., & Harrison, P. A. 1997, MNRAS, 289, 592
Lyne, A. G., & Manchester, R. N. 1988, MNRAS, 234, 477
Manchester, R. N., Hobbs, G. B., Teoh, A., & Hobbs, M. 2005, AJ, 129, 1993
Mandel, I., Müller, B., Riley, J., et al. 2021, MNRAS, 500, 1380
Noutsos, A., Schnitzeler, D. H. F. M., Keane, E. F., Kramer, M., & Johnston, S. 2013, MNRAS, 430, 2281
Philippov, A., Tchekhovskoy, A., & Li, J. G. 2014, MNRAS, 441, 1879
Postnov, K. A., & Kuranov, A. G. 2008, MNRAS, 384, 1393
Rankin, J. M. 1993a, ApJ, 405, 285
Rankin, J. M. 1993b, ApJS, 85, 145

[6] http://www.atnf.csiro.au/research/pulsar/psrcat, v. 1.68.

Sigurdsson, S. 2003, in ASP Conf. Ser. 302, Radio Pulsars, ed. M. Bailes, D. J. Nice, & S. E. Thorsett (San Francisco, CA: ASP), 391
Tauris, T. M., & Manchester, R. N. 1998, MNRAS, 298, 625
Verbunt, F., Igoshev, A., & Cator, E. 2017, A&A, 608, A57
Wang, C., Lai, D., & Han, J. L. 2006, ApJ, 639, 1007
Willcox, R., Mandel, I., Thrane, E., et al. 2021, ApJL, 920, L37
Yao, J., Zhu, W., Manchester, R. N., et al. 2021, NatAs, 5, 788
Zhang, L., Jiang, Z.-J., & Mei, D.-C. 2003, PASJ, 55, 461